Distortion Cancellation in Time-Stretch Analog-to-Digital Converter

Shalabh Gupta, *Student Member, IEEE*, George C. Valley, *Fellow, OSA*, and Bahram Jalali, *Fellow, IEEE*, *Fellow, OSA*

***Abstract*—We show that the symmetry properties of the two outputs from a push–pull Mach–Zehnder modulator can be exploited to reject dispersion-induced second-order distortions in the time-stretch analog-to-digital converter (TS-ADC). Using differential operation and signal processing in the digital domain, we experimentally demonstrate suppression of the signal harmonics generated due to system nonlinearities. Simulations predict that distortion-limited dynamic range improves from 34 to 57 dB. In addition, differential signaling improves the signal-to-noise ratio (SNR) by 3 dB and rejects an even-order nonlinear distortion added by an electronic digitizer in the TS-ADC. It is also shown that this approach is robust even in the presence of mismatches in the differential signal paths. In general, the approach can also be applied to any ultrawideband (multioctave) optical link to obtain a high dynamic-range system.**

***Index Terms*—Analog-to-digital conversion, electrooptic modulation, nonlinear distortion, optical communication, optical fiber dispersion.**

I. Introduction

DISPERSION-INDUCED second harmonics and intermodulation products are a serious problem in ultrawideband (multioctave) analog optical links [1], [2] and in systems that contain these links, such as the photonic time-stretch analog-to-digital converter (TS-ADC) [3]. In general, nonlinear distortion in analog optical links can be corrected by pre- or postdistortion circuits. However, since the dispersion-induced nonlinearity is frequency-dependent, electronic pre- or postdistortion cancellation is not effective in suppressing the nonlinear distortion produced by dispersion followed by square-law detection. Thus, most analog links operate at suboctave bandwidths or at low signal frequencies so that dispersion-induced harmonics and intermodulation components are negligible. Alternatively, costly solutions, such as dispersion-compensation fibers, can be employed. In systems such as the TS-ADC, dispersion plays the crucial role of reducing the bandwidth of the RF signal by stretching its waveform in time. However, in such systems, optical dispersion compensation does not work as it eliminates the fundamental stretching process itself.

Manuscript received March 3, 2007; revised August 9, 2007. This work was supported, in part, by The Aerospace Corporation's Independent Research and Development Program and, in part, by DARPA.

S. Gupta and B. Jalali are with the Optoelectronic Circuits and Systems Laboratory, Electrical Engineering Department, University of California, Los Angeles, CA 90095 USA (e-mail: shalabh@ee.ucla.edu; jalali@ucla.edu).

G. C. Valley is with The Aerospace Corporation, El Segundo, CA 90245 USA (e-mail: George.C.Valley@aero.org).

Color versions of one or more of the figures in this paper are available online at http://ieeexplore.ieee.org.

Digital Object Identifier 10.1109/JLT.2007.909343

Reduction of dispersion-induced second-order distortion is further complicated by the additional second-order distortion caused by the bias point drift of the Mach–Zehnder modulator, particularly in the case of chirped or tunable optical carriers [4]. Most wideband and high dynamic-range analog optical links are restricted to suboctave bandwidths to avoid second-order intermodulation components as well as to low modulation depths to avoid third and higher odd-order nonlinearities inherent in a Mach–Zehnder transfer function. Operation at low modulation depths is an unattractive solution in general because it limits power in the RF sidebands compared to the optical carrier, degrading the carrier-to-noise ratio (CNR). In this paper, we show that the dual outputs of a push–pull Mach–Zehnder modulator can be used differentially to cancel the distortion caused by the dispersion-induced nonlinearity in an analog optical link. Furthermore, additional postprocessing using an arcsine operation, which is performed in the digital domain [5], is shown to eliminate the frequency-independent nonlinearities caused by the modulator and by bias offsets. An application of this technique to a TS-ADC is also demonstrated.

II. Nonlinearities in Externally Modulated Analog Optical Links

Analog optical links are used in many applications, such as CATV distribution, antenna remoting, phased array antennas, and radio over fiber. Analog optical links also appear in many proposed photonic ADCs [6], including the TS-ADC. A large fraction of wideband analog optical links are externally modulated using Mach–Zehnder modulators because they have very high modulation frequencies, low loss, and high power-handling capability. The following sections describe two sources of the second-order nonlinear distortion that originate in the Mach–Zehnder modulators as well as methods to overcome them.

A. Dispersion-Induced Nonlinearities

The optical spectrum at the output of a Mach–Zehnder modulator contains the optical carrier, the upper and lower sidebands of the fundamental RF signal, and its harmonic and intermodulation components. At the detector, these sidebands and the optical carrier beat with each other, reproducing the RF signal plus its nonlinear-distortion components. In the absence of dispersion and perfect biasing, an even-order distortion cancels, yielding the well-known transfer function of the Mach–Zehnder modulator that has only the odd-order components. In the presence of dispersion, however, the even-order components appear,

and their intensity rapidly increases as the signal frequency and the amount of dispersion increase. For a multioctave system, this harmonic distortion can severely restrict the dynamic range.

The Mach–Zehnder modulators that use a directional coupler as the output combiner have two complementary output channels. Using a push–pull operation means that the modulated output fields have a zero chirp—a well-known property used in long-haul optical communications [7]. For such a modulator biased at quadrature, the output electric fields from the complementary output channels can be written as

$$E_{\pm}(t) = \frac{1}{\sqrt{2}} E_{\rm in}(t) \cos\left(\frac{\pi}{4} \pm \frac{m}{2} \cos \omega_{\rm RF} t\right) \tag{1}$$

where m is the modulation index, $E_{\rm in}(t)$ is the input electric field, and $\cos(\omega_{\rm RF} t)$ is the normalized RF-modulation signal. Using the mathematical framework described in [3], we find that the detector currents, after propagation of this field through a dispersive fiber of length L and group-velocity dispersion parameter β_2, can be written as

$$\begin{aligned} I_{\pm}(t) = I_{\rm Env}(t) \\ \times \Bigg[1 \mp m \cos\phi_{\rm DIP} \cos\omega_{\rm RF} t \\ + \frac{m^2}{8}(1 - \cos 4\phi_{\rm DIP}) \cos 2\omega_{\rm RF} t \\ \pm \frac{m^3}{96}(\cos 9\phi_{\rm DIP} + 3\cos 3\phi_{\rm DIP}) \cos 3\omega_{\rm RF} t + \cdots \Bigg] \end{aligned} \tag{2}$$

where $\theta_{\rm DIP} = \beta_2 \omega_{\rm RF}^2 L/2$, and $I_{\rm Env}(t)$ is the photodetector current in the absence of modulation.

Clearly, odd harmonics in the expressions for I_+ and I_- are 180° out of phase, whereas the even-harmonic components are in phase. Thus, taking the difference $I_+ - I_-$ removes all even-order nonlinear-distortion components. Fig. 1 shows the simulation results for a two-tone input signal with modulation index $m = 0.6$, fiber length $L = 15.5$ km, and $D = 17$ ps/nm/km ($\beta_2 = 21.67$ ps^2/km). Note that the dispersion-induced second-order harmonics are completely cancelled by using a differential operation. In practice, the cancellation is not perfect because of the amplitude and phase errors in the two signals, as discussed in Section V.

It must be emphasized that this cancellation takes place only for push–pull-type modulators that have zero signal chirp. For single-electrode modulators, which have chirped outputs, this operation fails as the dispersion behavior of the two output channels is no longer symmetric.

B. Nonlinearity Caused by Bias Drift

Mach–Zehnder modulators have small bias drifts due to temperature variations, stress, humidity, etc. [1]. While bias controllers can be employed to partially control the drifts, if the optical carrier is chirped or varied over a wide range of wavelengths, the bias offsets vary with optical wavelength [4] and are not easily controllable. These bias offsets introduce

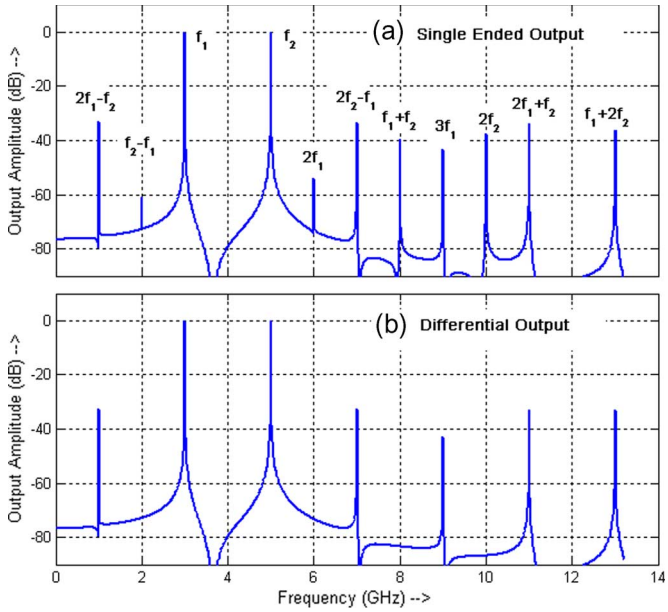

Fig. 1. Spectra of a two-tone test for an analog optical link with 3- and 5-GHz input frequencies and perfect Mach–Zehnder bias. (a) Single-ended output showing both second- and third-order distortion tones. (b) Output using differential operation showing that the dispersion-induced second-order distortion tones are rejected.

significant second-order distortions that are not corrected by the differential operation described in the previous section. If the Mach–Zehnder modulator is biased at the quadrature point with a small slowly time-varying bias offset $\delta(t)$, the two outputs I_+ and I_- after the RF modulation by signal $x(t)$, but without dispersion, can be written as

$$I_+(t) = I_{\rm Env}(t)\left[1 + \sin\left\{m \cdot x(t) + \delta(t)\right\}\right] \tag{3}$$

$$I_-(t) = I_{\rm Env}(t)\left[1 - \sin\left\{m \cdot x(t) + \delta(t)\right\}\right]. \tag{4}$$

These signals have third- and higher order distortions due to the sine function and a second-order nonlinearity caused by $\delta(t)$. The input RF signal can be recovered from the detector outputs by performing the following operation [5]:

$$I_{\rm out}(t) = \sin^{-1}\left[\frac{I_+ - I_-}{I_+ + I_-}\right] = m \cdot x(t) + \delta(t). \tag{5}$$

As discussed earlier, the differential operation removes the dispersion-induced second-order distortion. Division by $I_+ + I_-$ works as an averaging operation, scaling the output to make it independent of input intensity. It also helps in the rejection of optical intensity noise or any other multiplicative noise [8], [9].

The arcsine operation plays a crucial role in removing the third-order harmonic and intermodulation distortion components. High-pass filtering $I_{\rm out}(t)$ also removes the slowly varying bias offset $\delta(t)$ to give back the original RF signal $x(t)$. Fig. 2 shows the second-order distortion due to a bias error of 1° (even with differential operation) as well as the third-order distortion tones due to the Mach–Zehnder transfer function. These tones are suppressed by the arcsine operation. It should

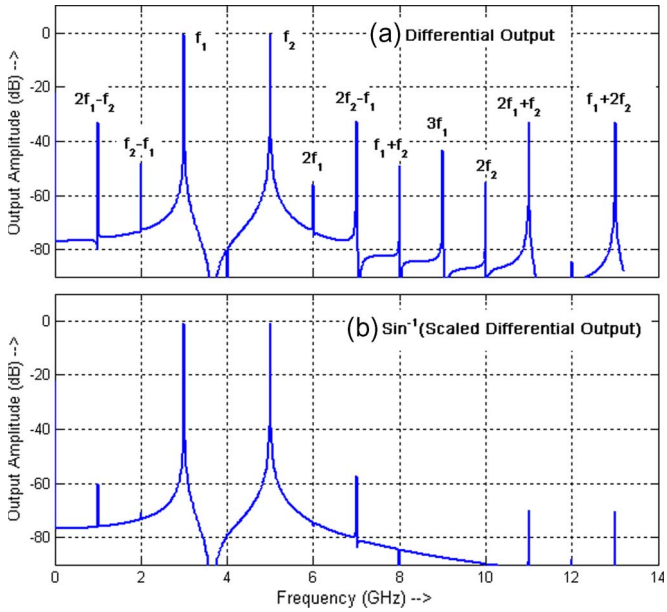

Fig. 2. Spectra for a two-tone test for an analog optical link with 3- and 5-GHz RF input frequencies. (a) Output amplitude as a function of frequency showing second- and third-order distortion tones caused by the Mach–Zehnder bias error and transfer characteristics. (b) Output spectrum with the distortions suppressed by the arcsine operation.

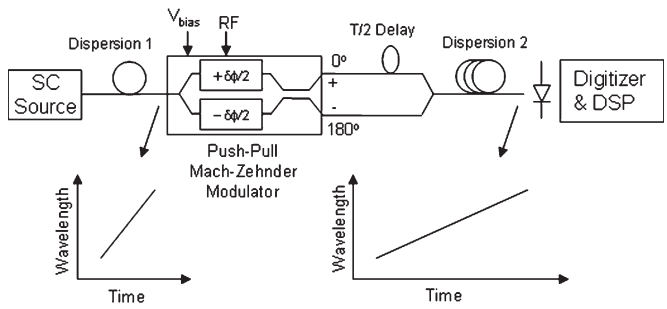

Fig. 3. TS-ADC with differential operation (SC = supercontinuum source).

be noted that (2) also shows the dispersion-induced third-order distortions, and for this reason, the arcsine operation is not able to provide a complete cancellation of the third-order distortions, which is in agreement with the simulations.

III. Time-Stretch Analog-to-Digital Conversion

The TS-ADC reduces the effective bandwidth of RF signals prior to digitization [10], [11]. To do this, the RF signal is modulated on a linearly chirped optical pulse. The propagation of a chirped waveform through a dispersive fiber stretches the pulse in the time domain and delivers a lower bandwidth signal to the electronic digitizer. Fig. 3 shows a realization of the TS-ADC system that uses the push–pull modulation and differential outputs. This system is used to experimentally demonstrate the distortion-suppression techniques, which are previously described in the context of conventional analog links. To simplify the hardware, the modulated optical pulses from the two Mach–Zehnder outputs are time-interleaved and combined on a single fiber. These pulses are then stretched in a dispersive fiber and converted to RF by a single photodetector.

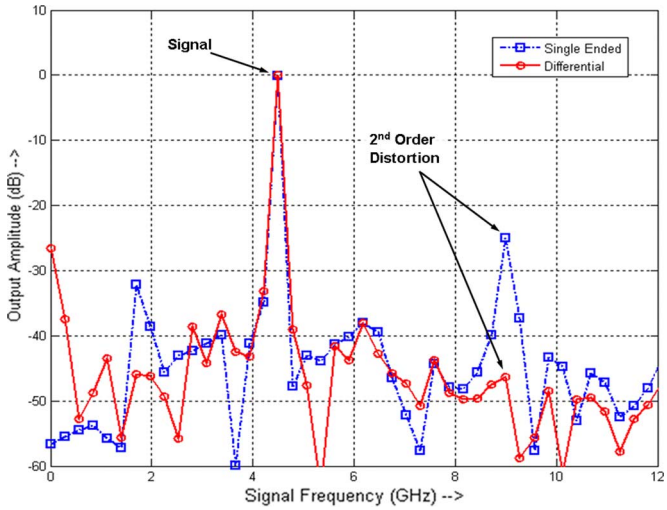

Fig. 4. Amplitude as a function of frequency for a 4.5-GHz RF input tone. The second harmonic at 9 GHz is suppressed by the differential operation. Note that the frequency scale corresponds to the original (prestretch) RF-signal frequency.

As in an analog optical link, the dispersion-induced nonlinear distortion can severely limit the dynamic range in the TS-ADC [3]. In particular, dispersion causes a rapid rise in the second-order distortion with an RF-signal frequency—a phenomenon that can restrict the operation of the ADC to suboctave bandwidths.

The inherent sinusoidal transfer function of the Mach–Zehnder modulator causes third- and higher order distortions. Bias fluctuations, which may be wavelength-dependent, are a second source of harmonic distortion. In the next section, we experimentally demonstrate that the differential operation followed by an arcsine correction can reduce the level of such distortions.

IV. Experimental Results

In the first experiment, the optical pulse was modulated with an RF signal at 4.5 GHz. The lengths of the dispersive fibers labeled Dispersion 1 and Dispersion 2 in Fig. 3 (L_1 and L_2) are chosen such that the dispersion effects are similar to the analog link simulated in Section II, and the stretch factor $1 + L_2/L_1$ is equal to 7.5. The modulation index m is set to the high value of about 0.85 to obtain a prominent dispersion-induced second harmonic tone. To obtain the desired differential operation, the two complementary pulses from the time-stretch output are aligned in time and subtracted in the digital domain. As can be seen in Fig. 4, the second harmonic tone, which is evident in the single-ended operation, is absent in the differential operation. In addition, a 3-dB improvement in SNR is observed, which is attributed to the coherent addition of the signal and the incoherent addition of noise [12]. The Mach–Zehnder bias offset was carefully kept low, and the second harmonic generated by it is below the noise floor of the Tektronix TDS7404 digitizer.

In the second experiment, the Mach–Zehnder modulator is intentionally biased with small offset from the quadrature

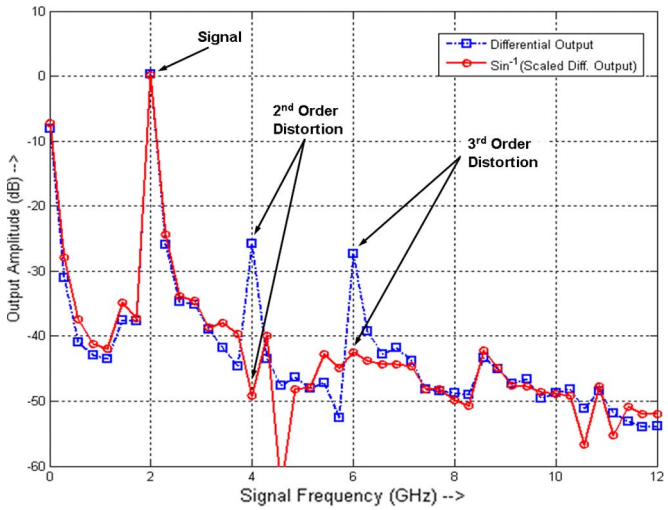

Fig. 5. Amplitude as a function of frequency for a 2-GHz input tone in a TS-ADC showing that the arcsine operation suppresses the second harmonic due to the Mach–Zehnder bias error and the third harmonic due to its transfer function. Note that the frequency scale corresponds to the original (prestretch) RF-signal frequency.

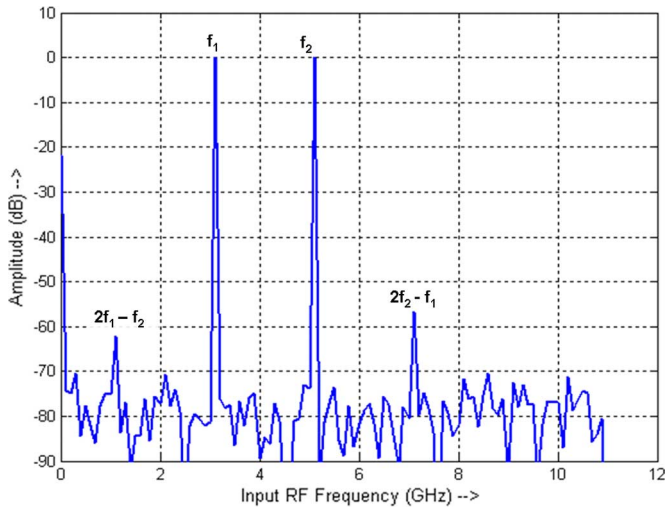

Fig. 6. Amplitude as a function of frequency calculated for a two-tone input with a 10-b electronic quantizer in a differential TS-ADC. Note that the frequency scale corresponds to the original (prestretch) RF-signal frequency.

point. The chirped optical carrier in the same time-stretch system is modulated with a 2-GHz RF tone. The digitized output spectrum shows harmonic tones at 4 and 6 GHz for the differential output. As shown in Fig. 5, the arcsine operation on the digitized output rejects harmonic tones to a level well below the noise floor.

In both experiments, the extent of distortion suppression that could be observed was limited by the noise floor of the digitizing scope used as the backend of the TS-ADC. If the noise floor of the backend digitizer can be significantly lowered, our technique is ultimately limited by the amplitude and phase errors in the differential outputs, which is analyzed in the next section. These two experiments demonstrate the potential of differential push–pull modulation to increase the dynamic range of the TS-ADC. It is important to note that the dispersion-induced second-order distortion may not be corrected by the commonly used distortion-cancellation techniques such as pre- or postdistortion in the electronic domain [13] since its behavior is frequency-dependent. In addition, as discussed earlier, the dispersion compensation is not possible in TS-ADCs, which renders the present approach more valuable in such systems.

V. Discussion

The TS-ADC is a favorable system for the implementation of the signal processing required by the algorithm described by (5) because the signal is already in the digital domain, and the required processing speed is reduced by the stretch factor. Since nonlinear distortions are reduced by this approach, the use of high modulation depths becomes possible—a fortuitous outcome which improves the CNR. This becomes crucial, particularly for wideband systems where the noise bandwidth is high. Therefore, its impact in terms of higher dynamic range is more significant in wideband multioctave systems.

A. Effects of Electronic Digitizer

Simulations of the TS-ADC were performed with a 10-b quantizer sampling the stretched RF signal at the Nyquist rate. The input RF signal is assumed to occupy a bandwidth of 1 to 11 GHz. With two tones at 3.1 and 5.1 GHz and a modulation index of 0.6, a signal-to-noise and distortion ratio (SINAD) of about 57 dB is calculated (see Fig. 6), under the assumption that the quantization errors limit the noise floor of the system. The SINAD is limited primarily by the third-order Mach–Zehnder modulator nonlinearity that is not perfectly cancelled by the arcsine operation.

A 10-b quantizer, which normally has a quantization noise floor of -61.7 dB with respect to a full-scale signal, now shows a quantization noise floor of -64.7 dB: a 3-dB improvement due to the differential operation. A practical electronic digitizer also adds a significant second-order distortion to the sampled RF signal.

The use of differential operation in the digital domain not only improves the SNR by 3 dB but also rejects the second-order distortion added by the electronic digitizer. As a result, the dynamic range of the digitizer also significantly improves by using the differential operation, which makes the use of the differential approach more attractive. For the same setup previously described, with an 8-b digitizer instead of 10-b digitizer, the simulation showed that 7.9 effective number of bits were obtained for the whole TS-ADC system, even when the detector output signal does not occupy the full scale of the digitizer because the modulation depth is only 0.6.

B. Effects of Phase and Amplitude Mismatches

The effectiveness of the differential approach can be limited by amplitude and phase mismatches between the two channels. While mismatches can be greatly reduced by a calibration of the system before the actual signal is sampled, it is important to quantify the effect of these mismatches.

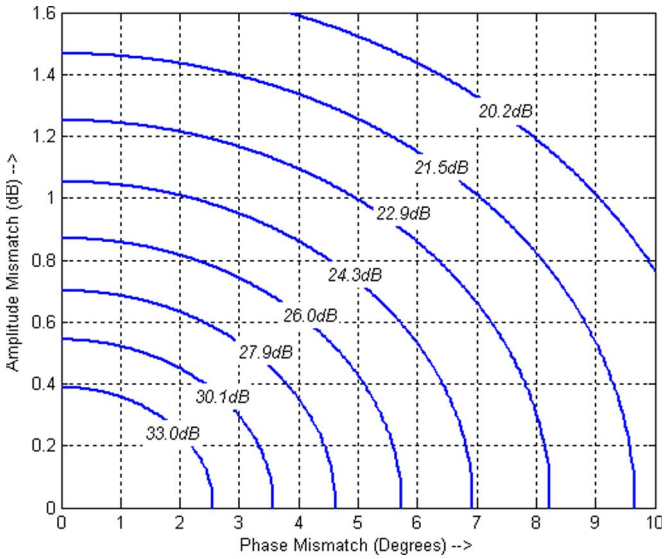

Fig. 7. Contour plots for DRRs that can be achieved as a function of amplitude and phase mismatches between the two differential channels.

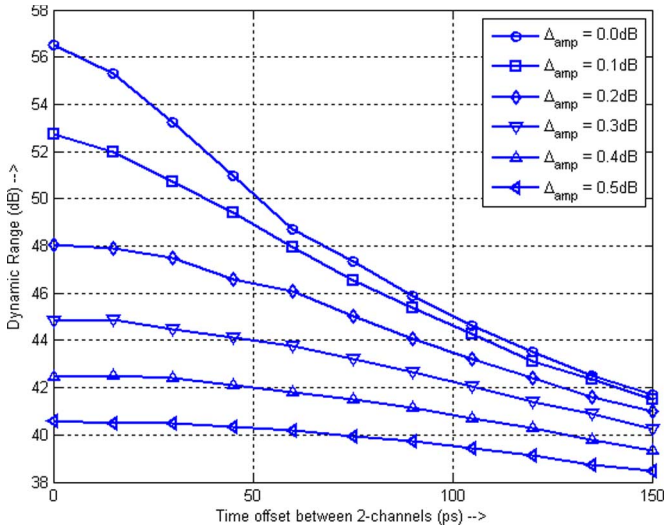

Fig. 8. Calculations of the dynamic range of the TS-ADC as a function of timing offsets between the two channels for different amplitude mismatch values.

For a sinusoidal signal with angular frequency ω, if the ratio of the current amplitudes in two channels is $\Delta_{\rm amp}$ (in decibels), and the phase difference between them is θ (in radians), then the two channel outputs can be written as

$$I_{\rm out1} = A(1+\delta/2)\cos(\omega t + \theta/2) \tag{6}$$

$$I_{\rm out2} = A(1-\delta/2)\cos(\omega t - \theta/2) \tag{7}$$

where $\Delta_{\rm amp} = 20\log((1+\delta/2)/(1-\delta/2))$ is the amplitude mismatch in a decibel scale.

If we consider this sinusoidal signal as the second-order distortion component, the distortion rejection ratio (DRR) can be defined as

$$\begin{aligned}\text{DRR} &= \frac{\langle (I_{\rm out1}+I_{\rm out2})^2\rangle}{\langle (I_{\rm out1}-I_{\rm out2})^2\rangle} \\ &= \frac{\left\langle [2\cos(\theta/2)\cos(\omega t) - \delta\sin(\theta/2)\sin(\omega t)]^2\right\rangle}{\left\langle [\delta\cos(\theta/2)\cos(\omega t) - 2\sin(\theta/2)\sin(\omega t)]^2\right\rangle} \\ &\approx \frac{4}{\delta^2+\theta^2}, \qquad (\text{for } \delta,\theta \ll 1)\end{aligned} \tag{8}$$

where $\langle \ldots \rangle$ indicates the time-averaged value.

The DRR indicates how well the distortion component is rejected by the differential operation. Fig. 7 shows contour plots for different rejection ratios as a function of phase and amplitude mismatch. It should be noted that the phase mismatch here corresponds to the mismatch between the phases of the stretched signals. In TS-ADC, the phase mismatch is reduced by the stretch factor for a particular timing offset between the two channels, since the signal frequency is lowered by the stretch factor. As a result, with differential operation and calibration, the dispersion-induced second-order distortion can easily be rejected to a value below the noise floor of the system.

The arcsine operation is also affected by the amplitude and phase mismatches between the two channels. Fig. 8 shows a plot of the dynamic range of the ADC in presence of the amplitude mismatches and timing offsets between the two channels, as predicted by simulations, for the two-tone test shown in Fig. 6. It should be noted that the x-axis in Fig. 8 is chosen to be the time offset instead of phase offset because the definition of the phase offset does not make much sense for a broadband signal. These mismatches can reduce the effectiveness of the approach to some extent, but one can expect very good results after calibration, which can easily be carried out in the digital domain.

VI. Conclusion

In this paper, we have shown that a push–pull Mach–Zehnder modulator with differential outputs can be used to cancel dispersion-induced second-order distortion. The differential approach, which is followed by an arcsine operation in digital domain, helps to obtain a high dynamic range for wideband (multioctave) optical links. In particular, this approach is very well suited to a multioctave operation of the TS-ADC system.

References

[1] W. I. Way, *Broadband Hybrid Fiber Coax Access System Technologies*. New York: Academic, 1998, ch. 7.

[2] G. K. Gopalakrishnan, T. J. Brophy, and C. Breverman, "Experimental study of fibre induced distortions in externally modulated 1550 nm analogue CATV links," *Electron. Lett.*, vol. 32, no. 14, pp. 1309–1310, Jul. 1996.

[3] Y. Han and B. Jalali, "Photonic time-stretched analog-to-digital converter: Fundamental concepts and practical considerations," *J. Lightw. Technol.*, vol. 21, no. 12, pp. 3085–3103, Dec. 2003.

[4] S. Dubovitsky, W. H. Steier, S. Yegnanarayanan, and B. Jalali, "Analysis and improvement of Mach–Zehnder modulator linearity performance for chirped and tunable optical carriers," *J. Lightw. Technol.*, vol. 20, no. 5, pp. 886–891, May 2002.

[5] J. C. Twichell and R. Helkey, "Phase-encoded optical sampling for analog-to-digital converters," *IEEE Photon. Technol. Lett.*, vol. 12, no. 9, pp. 1237–1239, Sep. 2000.

[6] G. C. Valley, "Photonic analog-to-digital converters," *Opt. Express*, vol. 15, no. 5, pp. 1955–1982, Mar. 2007.

[7] A. H. Gnauck, S. K. Korotky, J. J. Veselka, J. Nagel, C. T. Kemmerer, W. J. Minford, and D. T. Moser, "Dispersion penalty reduction using an

optical modulator with adjustable chirp," *IEEE Photon. Technol. Lett.*, vol. 3, no. 10, pp. 916–918, Oct. 1991.

[8] P. W. Juodawlkis, J. C. Twichell, G. E. Betts, J. J. Hargreaves, R. D. Younger, J. L. Wasserman, F. J. O'Donnell, K. G. Ray, and R. C. Williamson, "Optically sampled analog-to-digital converters," *IEEE Trans. Microw. Theory Tech.*, vol. 49, no. 10, pp. 1840–1853, Oct. 2001.

[9] Y. Han and B. Jalali, "Differential photonic time-stretch analog-to-digital converter," presented at the Lasers Electro-Optics Conf., Baltimore, MD, 2003, Paper CWH2.

[10] A. S. Bhushan, F. Coppinger, and B. Jalali, "Time-stretched analogue-to-digital conversion," *Electron. Lett.*, vol. 34, no. 11, pp. 1081–1083, May 1998.

[11] B. Jalali and F. Coppinger, "Data conversion using time manipulation," U.S. Patent 6 288 659, Sep. 11, 2001.

[12] D. Piehler, X. Zou, C. Y. Kuo, A. Nilsson, J. Kleefeld, G. Garcia, J. D. Ralston, and A. Mathur, "55 dB CNR over 50 km of fiber in an 80-channel externally-modulated AM-CATV system without optical amplification," *Electron. Lett.*, vol. 33, no. 3, pp. 226–227, Jan. 1997.

[13] R. Sadhwani and B. Jalali, "Adaptive CMOS predistortion linearizer for fiber-optic links," *J. Lightw. Technol.*, vol. 21, no. 12, pp. 3180–3193, Dec. 2003.

Shalabh Gupta (S'04) received the B.Tech. degree in electrical engineering from the Indian Institute of Technology, Kanpur, India, in 2001 and the M.S. degree in electrical engineering from the University of California, Los Angeles (UCLA), in 2004, where he is currently working toward the Ph.D. degree in electrical engineering with the Optoelectronic Circuits and Systems Laboratory, Electrical Engineering Department.

In August 2003, he was with Chrontel Inc., San Jose, CA, where he primarily designed analog integrated circuits for high-speed serial links. Before joining the Optoelectronic Circuits and Systems Laboratory while working toward for the Ph.D. degree, he was with Skyworks Solutions Inc., Irvine, CA, as a Senior Electrical Engineer, RFIC. At Skyworks, he contributed to the design and development of GSM/EDGE transceiver chipsets. His research focus is in the field of microwave photonics. His research interests include analog/RF integrated circuits, beam-forming antennas, and microwave photonics.

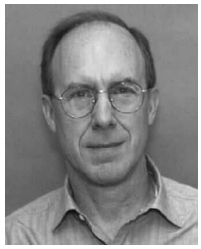

George C. Valley received the A.B. degree in physics from Dartmouth College, Hanover, NH, in 1966 and the Ph.D. degree in physics from The University of Chicago, Chicago, IL, in 1971.

He was with Cornell Aeronautical Laboratories, Ithaca, NY, from 1972 to 1977 and with Hughes Aircraft Company from 1977 to 1999. Since 1999, he has been a Senior Scientist with The Aerospace Corporation, El Segundo, CA. His past research has focused on nonlinear optics, optical solitons, photorefractive materials, free-space laser communication, and wave propagation in random media. His current research interests include optical fiber amplifiers, simulation of mixed-signal integrated circuits, and photonic analog-to-digital converters.

Dr. Valley is a member of the American Physical Society and a Fellow of the Optical Society of America.

Bahram Jalali (F'04) is currently a Professor of electrical engineering and the Director of the Optoelectronic Circuits and Systems Laboratory, Electrical Engineering Department, University of California, Los Angeles, (UCLA). From 1988 to 1992, he was a member of Technical Staff with the Physics Research Division, AT&T Bell Laboratories, Murray Hill, NJ, where he conducted research on ultrafast electronics and optoelectronics. While on leave from UCLA from 1999 to 2001, he founded Cognet Microsystems—a Los Angeles-based fiber-optic component company—where he served as the company's CEO, President, and Chairman from the company's inception through its acquisition by Intel Corporation in April 2001. From 2001 to 2004, he served as a Consultant with Intel Corporation. He has published over 200 scientific papers and holds six U.S. patents. His current research interests include silicon photonics and ultrafast photonic signal processing.

Dr. Jalali is a Fellow of the Optical Society of America (OSA), the Chair of the Los Angeles Chapter of the IEEE Lasers and Electro Optics Society, and a member of the California Nano Systems Institute. He serves on the Board of Trustees of the California Science Center. He received the BridgeGate 20 Award for his contribution to the Southern California economy. He was the recipient of the R.W. Wood Prize from the OSA. In 2005, he was chosen by *Scientific American Magazine* as one of the 50 Leaders Shaping the Future of Technology.